Convergent close-coupling method for positron scattering from noble gases

2012 New J. Phys. 14 035002

(http://iopscience.iop.org/1367-2630/14/3/035002)

New Journal of Physics
The open-access journal for physics

Convergent close-coupling method for positron scattering from noble gases

Dmitry V Fursa[1] **and Igor Bray**
ARC Centre for Antimatter–Matter Studies, Curtin University,
GPO Box U1987, Perth, WA 6845, Australia
E-mail: d.fursa@curtin.edu.au

New Journal of Physics **14** (2012) 035002 (18pp)
Received 29 November 2011
Published 1 March 2012
Online at http://www.njp.org/
doi:10.1088/1367-2630/14/3/035002

Abstract. We present the convergent close-coupling formulation for positron scattering from noble gases (Ne, Ar, Kr and Xe) within the single-center approximation. Target functions are described in a model of six p-electrons above an inert Hartree–Fock core with only one-electron excitations from the outer p^6 shell allowed. Target states have been obtained using a Sturmian (Laguerre) basis in order to model coupling to ionization and positronium (Ps) formation channels. Such an approach is unable to yield explicit Ps-formation cross sections, but is valid below this threshold and above the ionization threshold. The present calculations are found to show good agreement with recent measurements.

Contents

[1] Author to whom any correspondence should be addressed.

1. Introduction

Detailed understanding of positron scattering from atoms, ions and molecules is a difficult task for both theory and experiment. The relative scarcity of positrons compared to electrons makes it harder to develop experimental techniques. From a theoretical viewpoint, the interaction of positrons with matter is fundamentally different from electron interaction. While the absence of the exchange interaction makes the problem seemingly simpler, the addition of a new reaction channel, positronium (Ps) formation, brings a whole new set of problems.

Over the last decade, the development of more efficient positron sources led to renewed interest in positron–atom scattering. Detailed investigations by a number of groups have been performed on positron–helium scattering [1–9]. More recently, heavier noble gases (Ne, Ar, Kr and Xe) have been studied experimentally. Measurements of the grand total cross section, total ionization, direct ionization and Ps-formation cross sections [10–18] have been carried out. In addition, elastic scattering differential cross sections have been measured at a number of energies for Kr and Xe [13, 14, 19].

Previous theoretical work on positron scattering from noble gases (Ne, Ar, Kr and Xe) is mostly limited to various single-channel methods [20–23] that were applied to the calculation of elastic and grand total cross sections. These methods differ in the account of atomic polarizability and choice of optical potential used to model excitation and ionization channels. Note that no account of Ps-formation channels has been made in the construction of the optical potential. Additionally, positron impact excitation, ionization and Ps-formation cross sections have been calculated within a distorted wave method [24, 25]. We also note the many-body perturbation theory calculations [26] that have been useful in understanding the physics of the positron–atom interactions. None of these calculations show broad agreement with the experimental results, which, in turn, have also shown considerable variation.

A generally accurate account of Ps formation requires theoretical approaches that deal with the two-center (atom and Ps) nature of the collision process. Two-center formulations of the close-coupling (CC) method are the most successful approaches to the study of positron interactions with atoms. The technique relies on the expansion of the total wave function in the set of target states of the atom and Ps,

$$\Psi = \sum_a F_a(\boldsymbol{x}_0)\Phi_a(\boldsymbol{x}_1, \ldots, \boldsymbol{x}_N) + \mathcal{A}\sum_{bc} G_{bc}(\boldsymbol{R}_1)\phi_b(\boldsymbol{t}_1)\Phi_c^+(\boldsymbol{x}_1, \ldots, \boldsymbol{x}_{N-1}). \quad (1)$$

Here the first term is an expansion using the atomic $\Phi_a(\boldsymbol{x}_1, \ldots, \boldsymbol{x}_N)$ states, with $F_a(\boldsymbol{x}_0)$ being the positron channel functions. The second term represents an expansion in the Ps center $\phi_b(\boldsymbol{t}_1)$ states, $G_{bc}(\boldsymbol{R}_1)$ are the corresponding channel functions and the $\Phi_c^+(\boldsymbol{x}_1, \ldots, \boldsymbol{x}_{N-1})$ describe states of the residual ion. The antisymmetrization operator $\mathcal{A}$ ensures antisymmetry of the electrons in the residual ion and the Ps electron. Implementation of this method is a very difficult task, with only the simplest positron–hydrogen scattering system being solved to a high degree of accuracy [27, 28]. Even for the next simplest scattering system, positrons on helium, the two-center formulation relies on a number of approximations in order to make calculations feasible [1, 4, 5]. These approximations are concerned with evaluation of the exchange matrix elements between the electron in Ps and electron(s) in the residual ion. The error associated with such approximations is expected to be generally small, but of particular concern near the Ps-formation threshold.

The difficulty of performing two-center calculations for positron–atom scattering is well illustrated by positron scattering from noble gases (Ne, Ar, Kr and Xe). The only attempt to

perform such calculations was made nearly 20 years ago by McAlinden and Walters [29], who performed truncated coupled-static approximation calculations where only the ground states of the noble gas atom and Ps were retained.

A substantial simplification of the two-center CC method is the single-center CC approach. This method drops the second term in equation (1), and is only different by the sign of the projectile charge to the no-exchange CC calculations of electron–atom scattering. The ability of the single-center CC method to capture the physics of positron–atom scattering processes relies on a special choice of the target state expansion. It requires a so-called Sturmian basis that spans both the discrete and the continuous spectrum of the target atom. We would like to note that theoretical methods that make use of a Sturmian basis have been widely applied to electron–atom scattering. Among such methods are various implementations of the R-matrix with the pseudostates method [30–32], the J-matrix method [33–35] and the convergent CC (CCC) method [36–38].

The single-center CCC method does not account for Ps-formation channels explicitly. However, continuum-like pseudostates, obtained via Sturmian expansion, can model Ps-formation channels with high accuracy. For example, it was demonstrated for positron scattering from hydrogen [28] that two-center and single-center CC methods produce the same grand total and total ionization cross sections (TICS). The price one has to pay for simplicity of the single-center CC method is the slow convergence in the CC expansion due to the need to have target states with large values of orbital angular momentum. Such calculations are valid for the elastic scattering channel below the Ps-formation threshold, and for all channels above the ionization threshold where excitation of positive-energy states takes into account simultaneously the Ps-formation and ionization processes. However, in the region between the positronium formation threshold and ionization threshold, the present method fails as open positronium formation channels cannot be modeled via closed positive energy state channels. Given the high ionization thresholds of the noble gases, this approach is quite advantageous for low-energy scattering to determine the scattering length, see, for example, [10, 11].

The aim of this paper is to present a detailed formulation of positron scattering from the noble gases in the single-center formulation using the CCC method. This represents a major extension of the technique in that the active electron resides in the outer p^6 shell, requiring a very different approach from what was used previously. In the next section, the structure model used to describe the noble gases is presented, and the CC equations are formulated. Some selected results of the calculations are then presented to illustrate the accuracy and capabilities of the method.

2. Theory

We consider positron scattering from noble gases within the non-relativistic approximation. Single-center formulation of the non-relativistic CCC method has been used to perform scattering calculations. The CCC method has been extensively reviewed in our previous publications [39, 40]; here we present the relevant details of positron–noble gas scattering.

2.1. Noble gas structure calculations

We describe wave functions for the noble gases (Ne, Ar, Kr and Xe) by a model of six p-electrons above an inert Hartree–Fock core. Excited states of noble gases are obtained by

allowing one-electron excitations from the p^6 shell. In what follows we consider the more general case of one-electron excitation from a closed-shell atom with the outer shell electron occupying an orbital with angular momentum l_0, with $l_0 = 1$ being the case for noble gases. This model is similar to the frozen-core model of helium and can be obtained by setting $l_0 = 0$ in the present formulation. The helium frozen-core model has been used successfully in CCC calculations of e–He scattering [41], and this gives us confidence in the present approach.

In order to implement this structure model (taking Ne as an example) we perform calculations in a number of steps. First, we perform self-consistent Hartree–Fock calculations for the Ne^+ ion and obtain a set of orbitals: 1s, 2s, 2p. We will refer to 1s and 2s orbitals as inert core orbitals and to the 2p orbital as the frozen-core orbital.

The target atom Hamiltonian can be written in the standard form

$$H_t = \sum_{i=1}^{N} H_i + \sum_{i<j}^{N} V_{ij}, \tag{2}$$

where $N = 4l_0 + 2$ is the total number of electrons in the outer shell, V_{ij} is the Coulomb potential, and H_i is a quasi-one-electron Hamiltonian of the Ne^{5+} ion,

$$H_i = K_i + V_i^{\mathrm{HF}}. \tag{3}$$

Here K_i is the kinetic energy operator and V^{HF} is a non-local Hartree–Fock potential that is constructed using inert core orbitals φ_c (1s and 2s for Ne)

$$V^{\mathrm{HF}}\xi(\boldsymbol{r}) = -\frac{N}{r}\xi(\boldsymbol{r}) + \sum_{\varphi_c}\left(\int \mathrm{d}^3r' \frac{|\varphi_c(\boldsymbol{r}')|^2}{|\boldsymbol{r}'-\boldsymbol{r}|} - \frac{1}{r}\right)\xi(\boldsymbol{r}) - \sum_{\varphi_c}\int \mathrm{d}^3r' \frac{\varphi_c(\boldsymbol{r}')\xi(\boldsymbol{r}')}{|\boldsymbol{r}'-\boldsymbol{r}|}\varphi_c(\boldsymbol{r}). \tag{4}$$

The Hamiltonian (3) is diagonalized in the basis of Sturmian (Laguerre) functions [42],

$$\xi_\alpha(r) = \left(\frac{2\lambda_l(k-1)!}{(2l+1+k)!}\right)(2\lambda_l r)^{l+1}\exp(-\lambda_l r)L_{k-1}^{2l+2}(2\lambda_l r), \tag{5}$$

where $L_{k-1}^{2l+2}(2\lambda_l r)$ are the associated Laguerre polynomials with λ_l being the fall-off parameter, l is the orbital angular momentum and the index k ranges from 1 to N_l, the maximum number of Laguerre functions for a given value of the orbital angular momentum l. The result is a set of one-electron functions that satisfy

$$\langle\varphi_\alpha|H_i|\varphi_\beta\rangle = \epsilon_\alpha\delta_{\alpha,\beta}, \tag{6}$$

where $\delta_{\alpha,\beta}$ is the Kronecker delta symbol and ϵ_α is the one-electron energy.

The 2p orbital in the $\{\varphi_\alpha\}$ basis differs substantially from the Hartree–Fock 2p orbital. In order to build a one-electron basis suitable for the description of a neutral Ne atom, we replace the former orbital with the Hartree–Fock one. The basis is then orthogonalized by the Gram–Schmidt procedure. The resulting orthonormal basis is denoted by $\{\phi_\alpha\}$ and satisfies

$$\langle\phi_\alpha|H_i|\phi_\beta\rangle = e_{\alpha,\beta}. \tag{7}$$

The coefficients $e_{\alpha,\beta}$ can be trivially obtained from the one-electron energies ϵ_α and overlap coefficients between the Hartree–Fock 2p orbital and the $\{\varphi_\alpha\}$ basis.

The target states $\{\Phi_n\}$ of Ne are described via the configuration-interaction (CI) expansion

$$\Phi_n = \sum_\alpha C_\alpha^n\,\Phi_\alpha. \tag{8}$$

The set of configurations $\{\Phi_\alpha\}$ is built by angular momentum coupling of the wave function of $2p^5$ electrons and one-electron functions from the $\{\phi_\alpha\}$ basis. We will refer to the former wave function as the frozen-core wave function $\psi_c(l_0^{4l+1})$ and to the latter one as the active electron wave function. The frozen-core wave function has angular momentum l_0 and spin-1/2 and, when coupled with the active electron wave function ϕ_α, leads to a configuration with spin $s = 0, 1$, orbital angular momentum l ($|l_\alpha - l_0| \leqslant l \leqslant l_\alpha + l_0$) and parity $\pi = (-1)^{l_0+l_\alpha}$:

$$|\Phi_\alpha\rangle = \mathcal{A}\,|l_0^{N-1} : l_0\tfrac{1}{2}; l_\alpha : ls\pi\rangle, \tag{9}$$

where we used the fact that $N - 1 = 4l_0 + 1$. The antisymmetrization operator $\mathcal{A}$ is given by

$$\mathcal{A} = \frac{1}{\sqrt{N}}\left(1 - \sum_{i=1}^{N-1} P_{iN}\right), \tag{10}$$

where P_{ij} is a permutation operator. It is convenient to use the shorthand notation for the frozen-core wave function

$$|\bar{l}_0\rangle \equiv |l_0^{N-1} : l_0\tfrac{1}{2}\rangle.$$

With this notation an antisymmetric configuration (9) can be written as

$$|\Phi_\alpha\rangle = \mathcal{A}|\bar{l}_0; l_\alpha : ls\pi\rangle = \frac{1}{\sqrt{N}}\left(1 - \sum_{i=1}^{N-1} P_{iN}\right)|\bar{l}_0; l_\alpha : ls\pi\rangle. \tag{11}$$

The target orbital angular momentum l, spin s and parity π are conserved quantum numbers, and diagonalization of the target Hamiltonian is performed separately for each target symmetry $\{l, s, \pi\}$.

In the construction of configuration (9) we have assumed that the orbital ϕ_α is not the same as the frozen-core orbital (2p). The case when ϕ_α is equivalent to the frozen-core orbital corresponds to a closed shell configuration l_0^{4l+2} that has $l = 0$, $s = 0$ and $\pi = +1$,

$$|\Phi_0\rangle = |l_0^N : 00+\rangle = |\bar{l}_0; l_0 : 00+\rangle = |\bar{l}_0\rangle|l_0\rangle. \tag{12}$$

The set of configurations $\{\Phi_0, \Phi_\alpha\}$ form an orthonormal basis,

$$\langle\Phi_0|\Phi_0\rangle = 1, \quad \langle\Phi_0|\Phi_\alpha\rangle = 0, \quad \langle\Phi_\alpha|\Phi_\beta\rangle = \delta_{\alpha,\beta}.$$

In what follows, the relations $\mathcal{A}\,\mathcal{A} = \sqrt{N}\,\mathcal{A}$ and $\mathcal{A}|\Phi_0\rangle = \sqrt{N}\,|\Phi_0\rangle$ will be useful.

Our next task is to present expressions for the matrix elements of the target Hamiltonian in the basis of antisymmetric configurations (11) and (12). First we consider matrix elements of quasi-one-electron Hamiltonian,

$$\begin{aligned}\left\langle \Phi_\alpha \left| \sum_{i=1}^{N} H_i \right| \Phi_\beta \right\rangle &= \left\langle \bar{l}_0; l_\alpha : ls\pi \left| \sum_{i=1}^{N} H_i \left(1 - \sum_{j=1}^{N-1} P_{jN}\right) \right| \bar{l}_0; l_\beta : ls\pi \right\rangle \\ &= (N-1)\langle l_0|H_1|l_0\rangle\delta_{\alpha\beta} + \langle l_\alpha|H_N|l_\beta\rangle\delta_{l_\alpha l_\beta},\end{aligned} \tag{13}$$

$$\begin{aligned}\left\langle \Phi_0 \left| \sum_{i=1}^{N} H_i \right| \Phi_\alpha \right\rangle &= \sqrt{N}\left\langle \bar{l}_0; l_0 : 00+ \left| \sum_{i=1}^{N} H_i \right| \bar{l}_0; l_\alpha : 00+ \right\rangle \\ &= \sqrt{N}\delta_{l_0 l_\alpha}\,\langle l_0|H_N|l_\alpha\rangle,\end{aligned} \tag{14}$$

$$\left\langle \Phi_0 \left| \sum_{i=1}^{N} H_i \right| \Phi_0 \right\rangle = (N-1)\langle l_0|H_1|l_0\rangle + \langle l_0|H_N|l_0\rangle. \tag{15}$$

The term $(N-1)\langle l_0|H_1|l_0\rangle$ in equations (13) and (15) is an additive constant, and will be dropped as we require only the energy difference between target states. The remaining terms are given by equation (7).

We now turn to the calculation of matrix elements of the Coulomb interaction

$$V = \sum_{i<j=1}^{N} V_{ij}.$$

After some straightforward but tedious algebra, one can show that

$$\begin{aligned}\langle \Phi_\alpha|V|\Phi_\beta\rangle &= \left\langle \bar{l_0}; l_\alpha : ls\pi \left| V \left(1 - \sum_{i=1}^{N-1} P_{iN}\right) \right| \bar{l_0}; l_\beta : ls\pi \right\rangle \\ &= \delta_{\alpha,\beta} \left\langle \bar{l_0}; l_\alpha : ls\pi \left| \sum_{i<j=1}^{N-1} V_{ij} \right| \bar{l_0}; l_\beta : ls\pi \right\rangle \\ &+ \left\langle \bar{l_0}; l_\alpha : ls\pi \left| \sum_{i=1}^{N-1} (V_{iN} - V_{iN}P_{iN}) \right| \bar{l_0}; l_\beta : ls\pi \right\rangle, \end{aligned} \tag{16}$$

where the direct matrix element is given by

$$\begin{aligned}\left\langle \bar{l_0}; l_\alpha : ls\pi \left| \sum_{i=1}^{N-1} V_{iN} \right| \bar{l_0}; l_\beta : ls\pi \right\rangle &= \sum_{\kappa} F_\kappa(l_0, l_\alpha, l_0, l_\beta)\langle l_0\|C_\kappa\|l_0\rangle \ \langle l_\alpha\|C_\kappa\|l_\beta\rangle \\ &\times (-1)^{l_\alpha+l_0+L} \begin{Bmatrix} l_0 & l_\alpha & l \\ l_\beta & l_0 & \kappa \end{Bmatrix} \left[\delta_{\kappa 0}(N-1) - (-1)^\kappa(1-\delta_{\kappa 0})\right] \end{aligned} \tag{17}$$

and the exchange matrix element is

$$\begin{aligned}\left\langle \bar{l_0}; l_\alpha : ls\pi \left| \sum_{i=1}^{N-1} V_{iN}P_{iN} \right| \bar{l_0}; l_\beta : ls\pi \right\rangle &= \sum_{\kappa} F_\kappa(l_0, l_\alpha, l_\beta, l_0)\langle l_\alpha\|C_\kappa\|l_0\rangle \ \langle l_0\|C_\kappa\|l_\beta\rangle \\ &\times \left[\frac{1}{2l_\alpha+1}\delta_{l_\alpha l_\beta} - \frac{2(-1)^{l_\alpha+l_\beta}}{2l+1}\delta_{kl}\delta_{s0}\right]. \end{aligned} \tag{18}$$

Here quantities C_{kq} are related to the spherical harmonics Y_{kq} as

$$C_{\kappa\mu} = \sqrt{\frac{4\pi}{2\kappa+1}} Y_{\kappa\mu} \tag{19}$$

and its reduced matrix element is

$$\langle l\|C_\kappa\|l'\rangle = \hat{l'}\, C^{000}_{l'\kappa l}, \tag{20}$$

where $\hat{l} = \sqrt{2l+1}$ and $C^{m_1 m_2 M}_{l_1 l_2 L}$ is a Clebsch–Gordan coefficient.

The radial two-electron Coulomb integrals are defined as

$$F_\kappa(l_\alpha, l_\beta, l_\delta, l_\gamma) = \iint \mathrm{d}r_1\, \mathrm{d}r_2 \frac{r_<^\kappa}{r_>^{\kappa+1}} \phi_\alpha(r_1)\phi_\beta(r_2)\phi_\gamma(r_1)\phi_\delta(r_2). \tag{21}$$

The matrix elements involving the Φ_0 configuration are

$$\begin{aligned}\langle \Phi_0|V|\Phi_\alpha\rangle &= \sqrt{N}\langle \bar{l}_0, l_0 : 00+|V|\bar{l}_0, l_\alpha : ls\pi\rangle \\ &= \sqrt{N}\left\langle \bar{l}, l : 00+\left|\sum_{i=1}^{N-1} V_{iN}\right|\bar{l}, l_\alpha : 00+\right\rangle \delta_{ll_\alpha}\delta_{l0}\delta_{s0}\end{aligned} \tag{22}$$

and

$$\begin{aligned}\langle \Phi_0|V|\Phi_0\rangle &= \langle \bar{l}_0, l_0 : 00+|V|\bar{l}_0, l_0 : 00+\rangle \\ &= \left\langle \bar{l_0}, l_0 : 00+\left|\sum_{i<j=1}^{N-1} V_{ij}\right|\bar{l}_0, l_0 : 00+\right\rangle + \left\langle \bar{l}_0, l_0 : 00+\left|\sum_{i=1}^{N-1} V_{iN}\right|\bar{l}_0, l_0 : 00+\right\rangle.\end{aligned} \tag{23}$$

The right-hand side of equation (22) and the second term on the right-hand side of equation (23) are evaluated with the help of equation (17). The first terms on the right-hand side of equations (16) and (23) are equal. They just lead to a shift of energy, and will be dropped.

With matrix elements of the target Hamiltonian (2) in the basis of configurations (11) and (12) evaluated, we solve the standard eigenvalue problem for each target symmetry (total angular momentum l, total spin s and total parity π), and obtain a set of target states that satisfy

$$\langle \Phi_n|H_t|\Phi_m\rangle = \delta_{n,m}\epsilon_n, \tag{24}$$

where ϵ_n is the target state energy. For positron scattering from the ground state ($s = 0$) of a noble gas atom, only target states with $s = 0$ can be excited. The size of the calculations can be increased by simply increasing the number of Laguerre functions (N_l). Low-lying states will converge to bound states of the target, while the remaining (pseudo) states will provide an increasingly accurate representation of the target atom high-lying bound states and an increasingly dense square-integrable representation of the target continuum.

2.2. Scattering calculations

The total Hamiltonian of the positron and target atom scattering system can be written as

$$H = K_0 + V_0 + \sum_{i=1}^{N} V_{0i} + H_\mathrm{t}, \tag{25}$$

where the index '0' indicates the positron coordinates. The potential V_0 describes the interaction of the positron with the inert core (Ne^{5+})

$$V_0 = \frac{N}{r_0} + U_0, \tag{26}$$

where

$$U_0 = \sum_{\varphi_\mathrm{c}} \left(\frac{1}{r} - \int \mathrm{d}^3 r' \frac{|\varphi_\mathrm{c}(\boldsymbol{r}')|^2}{|\boldsymbol{r}' - \boldsymbol{r}|}\right). \tag{27}$$

The single-center CCC method solves the Schrödinger equation

$$H\Psi^{(+)} = E\Psi^{(+)}, \tag{28}$$

where E is the total energy of the scattering system, by expanding the total scattering wave function Ψ in a large set of target states

$$\Psi^{(N+)} = \sum_{n=1}^{N} F_n^{(+)}(\boldsymbol{r}_0)\Phi_n(\boldsymbol{r}_1, \ldots, \boldsymbol{r}_N), \tag{29}$$

where $F_n^{(+)}(\boldsymbol{r}_0)$ is a positron channel function. Substituting the expansion (29) in the Schrödinger equation (28) leads to a set of coupled Lippmann–Schwinger equations,

$$\langle \boldsymbol{k}_f^{(-)}\Phi_f|T_N|\Phi_i\boldsymbol{k}_i^{(+)}\rangle = \langle \boldsymbol{k}_f^{(-)}\Phi_f|V|\Phi_i\boldsymbol{k}_i^{(+)}\rangle + \sum_{n=1}^{N}\int \mathrm{d}^3k \frac{\langle \boldsymbol{k}_f^{(-)}\Phi_f|V|\Phi_n\boldsymbol{k}^{(-)}\rangle\langle \boldsymbol{k}^{(-)}\Phi_n|T_N|\Phi_i\boldsymbol{k}_i^{(+)}\rangle}{E^{(+)} - \varepsilon_k - \epsilon_n}. \tag{30}$$

The T-matrix is defined to be

$$\langle \boldsymbol{k}_f^{(-)}\Phi_f|T_N|\Phi_i\boldsymbol{k}_i^{(+)}\rangle = \langle \boldsymbol{k}_f^{(-)}\Phi_f|V|\Psi_i^{(N+)}\rangle \tag{31}$$

and the potential V is given by

$$V = V_0 + \sum_{i=1}^{N} V_{0i} - U, \tag{32}$$

where U is an arbitrary short-ranged distorting potential. The final calculated T-matrix should be independent of the choice of U. We note that matrix elements in equation (30) are diagonal in the positron and target atom spin quantum numbers. Hence, we have dropped all spin notation.

The positron continuum waves $|\boldsymbol{k}\rangle$ may be plane ($U = 0$) waves, or distorted waves as solutions of the following equation:

$$(K_0 + U - \epsilon_k)\,|\boldsymbol{k}^{(\pm)}\rangle = 0. \tag{33}$$

A convenient choice for U is

$$U = V_0 + \left\langle \Phi_{\mathrm{gs}} \left| \sum_{i=1}^{N} V_{0i} \right| \Phi_{\mathrm{gs}} \right\rangle, \tag{34}$$

where Φ_{gs} is the ground state wave function of the target atom. In the partial-wave expansion

$$\langle \boldsymbol{r}|\boldsymbol{k}^{(\pm)}\rangle = (2/\pi)^{1/2}(kr)^{-1}\sum_{L,M} i^L\, \mathrm{e}^{\pm \mathrm{i}\delta_L} u_L(k, r)Y_{LM}(\hat{\boldsymbol{r}})Y_{LM}^*(\hat{\boldsymbol{k}}), \tag{35}$$

where $u_L(k, r)$ are real regular solutions of equation (33).

We solve the coupled Lippmann–Schwinger equations for the T matrix by expanding (30) in partial waves J of the total orbital angular momentum and parity Π. The reduced V (or T) matrix elements are defined by

$$\langle Lk^{(-)}, n\pi l\|V_\Pi^J\|n'\pi' l', L'k'^{(+)}\rangle = \sum_{M,m,M',m'} C_{LlJ}^{MmM_J} C_{L'l'J}^{M'm'M_J} \int \mathrm{d}\hat{\boldsymbol{k}} \int \mathrm{d}\hat{\boldsymbol{k}}' Y_{L'M'}(\hat{\boldsymbol{k}}')Y_{LM}^*(\hat{\boldsymbol{k}}) \times \langle \boldsymbol{k}^{(-)}\Phi_n^{\pi lm}|V|\Phi_{n'}^{\pi' l' m'}\boldsymbol{k}'^{(+)}\rangle. \tag{36}$$

Here we use the coupled angular momentum form for the positron–atom wave function

$$\langle \boldsymbol{r}|Lk^{(\pm)}, n\pi l : J\Pi\rangle = (2/\pi)^{1/2}(kr_0)^{-1} i^L \, \mathrm{e}^{\pm \mathrm{i}\delta_L} u_L(kr_0) \sum_{M,m} C^{MmM_J}_{LlJ} Y_{LM}(\hat{\boldsymbol{r}}) \Phi^{\pi lm}_n. \tag{37}$$

The multipole expansion of the potential (32) is given by

$$V = \sum_{i=1}^{N} \sum_{\lambda,\mu} v_\lambda(r_0, r_i) C^*_{\lambda\mu}(\boldsymbol{r}_0) C_{\lambda\mu}(\boldsymbol{r}_i), \tag{38}$$

where

$$v_\lambda(r_0, r_1) = \delta_{\lambda 0}\,(V_0 - U) - \frac{r^\lambda_<}{r^{\lambda+1}_>}. \tag{39}$$

Calculation of the reduced matrix elements of the potential V can be performed with the help of standard techniques of angular momentum algebra. As a first step we use the CI expansion (8) to express these matrix elements via matrix elements for configurations $\{\Phi_\alpha\}$

$$\langle Lk^{(-)}, n\pi l \| V^J_\Pi \| n'\pi' l', Lk^{(+)}\rangle = \sum_{\alpha\beta} C^n_\alpha C^{n'}_{\alpha'} \langle Lk^{(-)}, \alpha\pi l \| V^J_\Pi \| \alpha'\pi' l', L'k'^{(+)}\rangle. \tag{40}$$

Next we use the multipole expansion of the potential (38) to obtain

$$\langle Lk^{(-)}, \alpha\pi l \| V^J_\Pi \| \alpha'\pi' l', L'k'^{(+)}\rangle = \frac{2}{\pi k k'} i^{L'-L} \, \mathrm{e}^{\mathrm{i}\delta_L} \, \mathrm{e}^{\mathrm{i}\delta_{L'}} \sum_\lambda (-1)^{l+L'+J} \begin{Bmatrix} L & l & J \\ l' & L' & \lambda \end{Bmatrix}$$
$$\times \langle L \| C_\lambda \| L'\rangle (A_\lambda + B_\lambda). \tag{41}$$

Here the coefficients A_λ and B_λ are given by

$$A_\lambda = \langle \phi_{\alpha'} | \phi_\alpha \rangle \hat{l}\hat{l}' (-1)^{l_0+l_\alpha+l'+\lambda} \begin{Bmatrix} l_\alpha & l_0 & l \\ l_\beta & l' & l_0 \end{Bmatrix} \langle l_0 \| C_\lambda \| l_0 \rangle \left[(N-2)\delta_{\lambda,0} + 1\right] F_\lambda(L, l_0, L', l_0) \tag{42}$$

and

$$B_\lambda = (1 + (\sqrt{N} - 1)|\delta_{\alpha,0} - \delta_{\alpha',0}|)\, \hat{l}\hat{l}' (-1)^{l_0+l+\lambda+l_{\alpha'}} \begin{Bmatrix} l_0 & l & l_\alpha \\ \lambda & l_{\alpha'} & l' \end{Bmatrix} [\langle l_\alpha \| C_\lambda \| l_{\alpha'}\rangle]\, F_\lambda(L, l_\alpha, L', l_{\alpha'}). \tag{43}$$

We note that for the case involving Φ_0 configuration ($\alpha = \alpha' = 0$) the above expressions simplify to

$$A_\lambda + B_\lambda = \delta_{\lambda,0} N F_\lambda(L, l_0, L', l_0). \tag{44}$$

The Lippmann–Schwinger equation for the reduced T-matrix is solved by reducing it to a set of linear equations [40]. The resulting T-matrix is used to obtain scattering amplitudes and cross sections for the transitions of interest.

3. Results

We have performed CCC calculations of positron scattering from noble gases using CC expansions that are detailed in table 1. The maximum value of the target orbital angular momentum was chosen to be $l_{\max} = 8$, which was sufficient to obtain convergence in the scattering calculations (where they are formally valid). As we have discussed earlier, an account

Table 1. Size of the CC expansion of the CCC calculations. N is the number of states and l_{max} is their maximum orbital angular momentum.

Atom	N	l_{max}
Ne	233	8
Ar	334	8
Kr	502	8
Xe	502	8

Table 2. Ionization energies (eV) for He, Ne, Ar, Kr and Xe atoms obtained in the frozen-core CCC calculations. Experimental levels listed by NIST [47] are also shown.

Atom	CCC	Experiment
He	23.74	24.59
Ne	20.57	21.56
Ar	14.95	16.76
Kr	13.38	14.00
Xe	11.73	12.13

of Ps-formation channels in single-center CC calculations relies on an adequate discretization of the target continuum. This suggests a Sturmian basis (5) with relatively small exponential fall-off parameters (more diffuse functions). On the other hand, representation of the bound-state spectrum invites a Sturmian basis with larger exponential fall-off parameters (short-range functions), particularly for the heavier atoms. The way for us to satisfy these competing requirements is to increase the number of Sturmian functions N_l used in the diagonalization. This has the consequence of increasing the CC expansion as we go from lighter to heavier noble gas atoms.

One measure of the accuracy of the structure model we use in the CCC calculations is the comparison of calculated and observed ionization energies that are presented in table 2. The CCC result for helium was also obtained within the frozen-core model. Such a model produces a similar level of accuracy for all of the considered targets.

Another important requirement for the target state basis is the ability to obtain the correct value of static dipole polarizability, which can particularly influence the scattering results at the lower energies. We adjust the polarizability arising in the frozen-core model by utilizing a model polarization potential that modifies the dipole term of the electron–electron Coulomb potential using the following expression [43, 44]:

$$V_{\rm pol}(\boldsymbol{r}_i, \boldsymbol{r}_j) = -\frac{\alpha}{r_i^3 r_j^3}(\boldsymbol{r}_i, \boldsymbol{r}_j)\, W(r_i/\rho)\, W(r_j/\rho), \tag{45}$$

where

$$W(r/\rho) = \sqrt{1 - \mathrm{e}^{-(r/\rho)^6}}. \tag{46}$$

The dipole part of the positron–electron Coulomb potential is modified similarly using $-V_{\rm pol}(\boldsymbol{r}_0, \boldsymbol{r}_j)$.

Table 3. Experimental static dipole polarizability α_d (a.u.) for Ne, Ar, Kr and Xe atoms, and the values of ρ to achieve them in the frozen-core structure model, see equation (45).

Atom	ρ	Experiment
Ne	3.55	2.67
Ar	4.68	11.1
Kr	5.45	17.1
Xe	6.50	27.8

The above modification of the Coulomb potential requires calculation of the optical oscillator strength using the modified expression for the dipole–length transition operator [45, 46]

$$\boldsymbol{r}' = \boldsymbol{r}\left[1 - \frac{\alpha}{r^3}\, W(r/\rho)\right]. \tag{47}$$

The static dipole polarizability can be obtained as

$$\alpha_d = \sum_n f_n/(2\epsilon_n)^2, \tag{48}$$

where f_n is the optical oscillator strength for the transition to the state Φ_n from the ground state, ϵ_n is the corresponding excitation energy, and summation is over both negative and positive energy ^1P states.

We take α to be the experimental value as given in table 3, and the parameter ρ is chosen to yield this experimental value of α_d in the CCC structure model, equation (48). We have no *ab initio* reason to choose α as we have, and have done so simply to reduce the number of free parameters from two (α and ρ) to one (ρ). Note that a major part of the polarizability comes from the continuum part of the spectrum. This signifies the importance of performing an adequate discretization of the target continuum.

The effect of the static dipole polarizability at the lower energies is well illustrated in figure 1, where differential cross sections for elastic scattering of positrons from the ground state of Xe are presented. At low energies of 1 eV the present CCC calculations are in good agreement with the relativistic optical potential (ROP) calculations of McEachran *et al* [14]. Both of these theoretical models have a static dipole polarizability in good agreement with experiment [14]. This contrasts with the polarized-orbital calculations of Sin Fai Lam [21] who has used a less accurate account of atomic polarizability.

At the higher positron energy of 15 eV, which is above the Ps-formation threshold, we find substantial differences between CCC and ROP with the CCC results in better agreement with the experiment. Here the major difference between CCC and ROP is in the account of the Ps-formation channel within the CCC method (when above the ionization threshold). Interestingly, the account of such additional reaction channels leads to an enhancement of forward scattering.

The grand total cross sections for positron scattering from Ne, Ar, Kr and Xe are presented in figure 2. This cross section is a sum of elastic, excitation, direct ionization and Ps-formation cross sections. For all target atoms the cross sections have similar features. They have a plateau at the presented larger positron energies and a minimum at low energies below the Ps-formation threshold. This minimum is very sharp for Ne and becomes progressively shallower for the

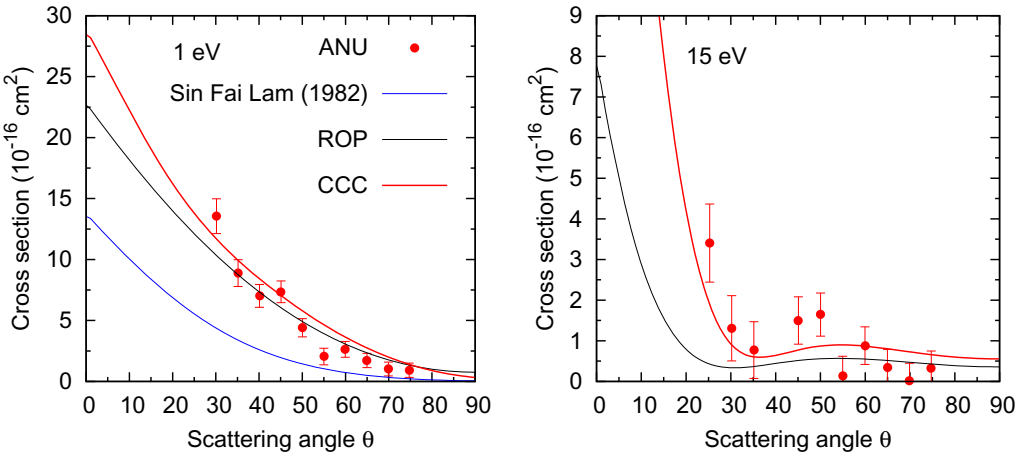

Figure 1. Elastic differential cross section for positron scattering from Xe. The experimental results are from the work [14]. The present CCC calculations are described in the text. Other theoretical results are from the work [14] ROP and [21].

heavier noble gas atoms. The sharp minimum for Ne TCS at low energies is due to a minimum in S-wave scattering while all higher partial wave cross sections are negligible and, therefore, it is an example of a Ramsauer–Townsend minimum. At very small energies the cross section rises very sharply, indicating the existence of a virtual level for the positron. We note also the rapid rise of the cross sections as Ps-formation channels open.

There is some scatter in the experimental data for grand total cross sections. Similarly, previous theoretical calculations (all of them are single-channel methods) show large variations depending on the accuracy with which the polarization potential is modeled. See [12–14] for detailed discussions and note only that here the CCC calculations are in very good agreement with the measurements taken by the ANU and Trento groups. The region between Ps-formation and ionization thresholds where the single-center CCC method cannot describe the scattering has been excluded from the calculations.

The interaction of positrons with atoms at low energies is of particular interest. The possibility of positron binding to atoms has been investigated theoretically in [58] (see also [59] for a useful discussion). It depends on the interplay of short-range electrostatic repulsion from the atomic center and long-range attraction due to the polarization potential. In addition, for noble gases the virtual Ps-formation channels produce effective short-range attraction. The scattering length a is useful in understanding the physics of the scattering process at low energies. Repulsive potentials lead to a positive scattering length, while attractive potentials lead to a negative scattering length. In calculations, the sign and absolute value of the scattering length can be easily obtained from the low-energy behavior of the S-wave phase shifts

$$\delta_0(k) = -ak, \tag{49}$$

where k is the positron momentum.

For low-energy positron scattering from noble gases the overall interaction potential is attractive as can be seen from the scattering length values presented in table 4. As we go from the lighter Ne atom to the heavier Ar, Kr and Xe atoms the scattering length grows in absolute value significantly. This is consistent with a large increase in the static dipole polarizability, see

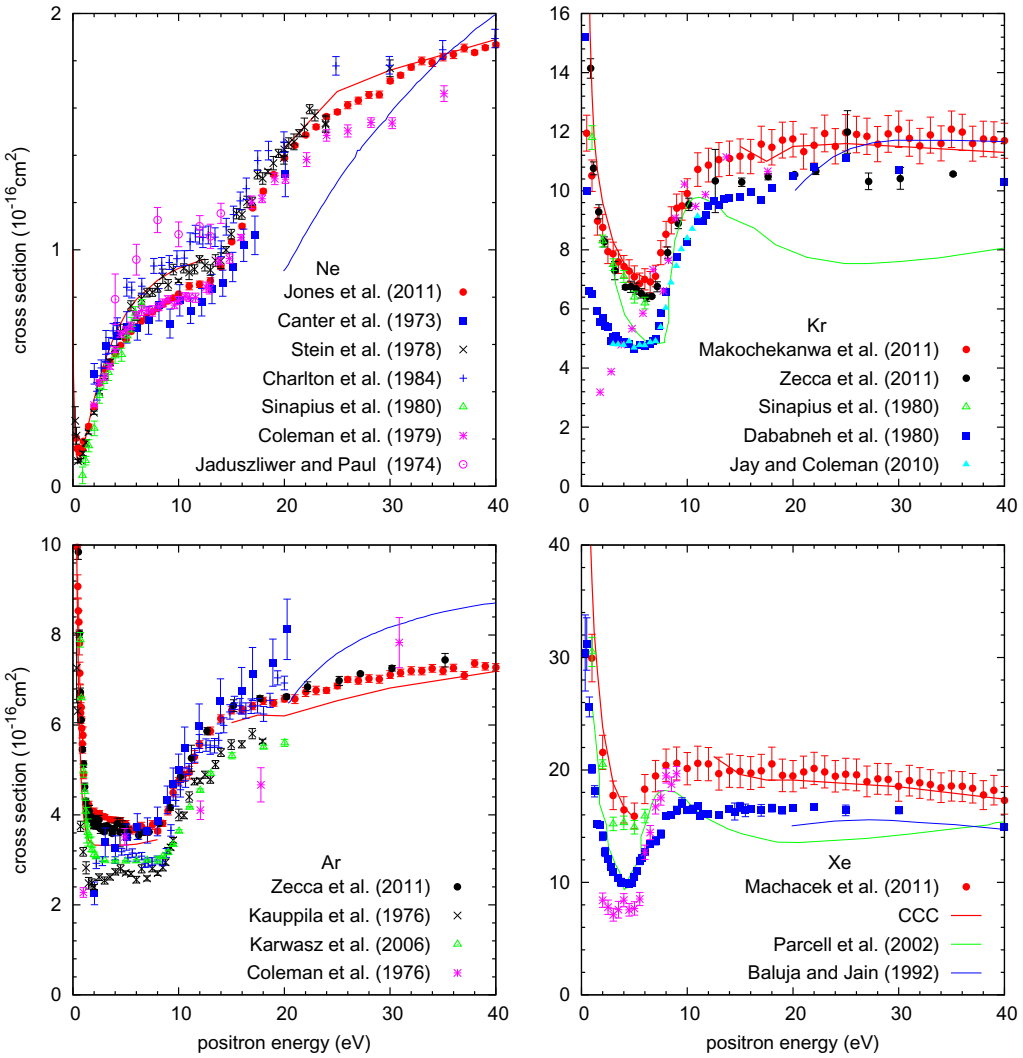

Figure 2. Grand total cross section for positron scattering from Ne, Ar, Kr and Xe. The experimental data are from [10–14, 48–57]. The present theory is labeled as CCC, and the other theory is from [22, 23].

table 3. Large values of the scattering length for Ar, Kr and particularly for Xe mean that the zero-energy elastic cross section,

$$\sigma = 4\pi a^2, \tag{50}$$

is very large. This can be seen in figure 3 where we present calculations performed at the energies where the cross section converges to the constant value given by the equation (50). We find good agreement between the present CCC calculations and MBPT results of [60] for all the considered noble gas atoms, while the agreement with the POM of [61] is less satisfactory, particularly for Xe. Recent experimental estimates, with the aid of the CCC theory, of the scattering length by Zecca *et al* [10, 11] are in good agreement with all of the theoretical values.

Given the sensitivity of the calculated scattering length to the static dipole polarizability, it is necessary to have this correct, but unfortunately this is not sufficient. In our case we utilized equation (45) to yield the required polarizability in a phenomenological way. By

Table 4. Scattering length (a.u.) for Ne, Ar, Kr and Xe atoms. Polarized orbital model (POM) calculations are from [61], many-body perturbation theory (MBPT) calculations are from [60] and experiments (aided by the CCC calculations) are from [10, 11].

Atom	CCC	MBPT	POM	Experiment
Ne	−0.53	−0.43	−0.61	
Ar	−4.3	−4.4	−5.3	-4.9 ± 0.7
Kr	−11.2	−10.2	−10.4	-10.3 ± 1.5
Xe	−117	−81	−45	

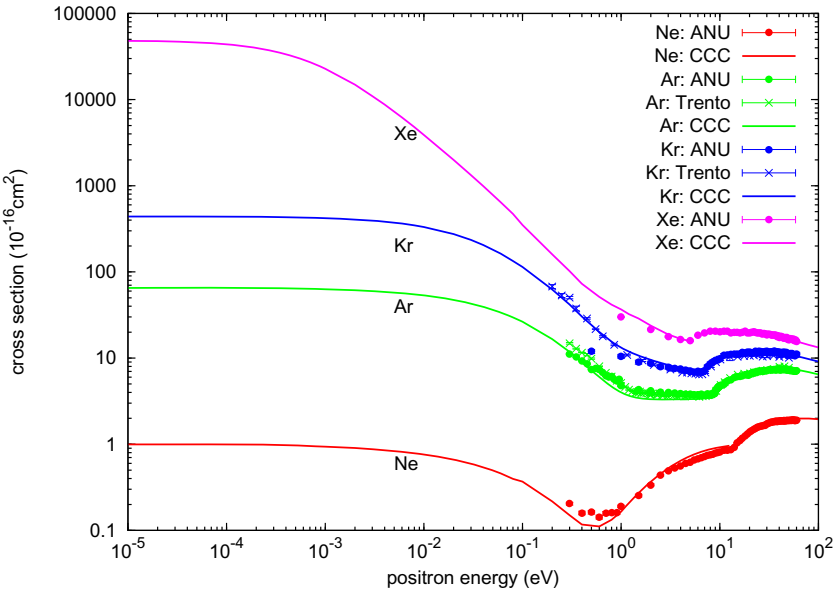

Figure 3. Grand total cross section for positron scattering from Ne, Ar, Kr and Xe. Experiments are due to the ANU [12–14] and Trento [10, 11] groups.

changing the parameters we are able to yield the same polarizability, but different cross sections. Consequently, there is some uncertainty associated with the presented results. Relaxing the frozen-core model is considerably more difficult than in the helium case [41], but is necessary for reducing the uncertainty of the scattering length calculations. Away from low energies the sensitivity to the choice of parameters in equation (45) diminishes.

The single-center CCC method allows us to obtain an estimate of the TICS from the excitation cross sections for positive-energy states. Note that the CCC-calculated TICS is non-zero only above the ionization threshold by construction, while the experimental TICS is a sum of direct ionization and Ps-formation cross sections. In figure 4, we present a comparison of the CCC results with the TICS values measured in [16], as well as direct ionization cross sections measured in [17, 18], and Ps-formation cross sections measured by the UCSD [15] and ANU [12–14] groups. The sharp rise of the CCC-calculated TICS at the ionization threshold is in contrast with the threshold behavior of TICS for electron–atom scattering, which behave more like the measured direct ionization cross sections presented in figure 4. The reason for

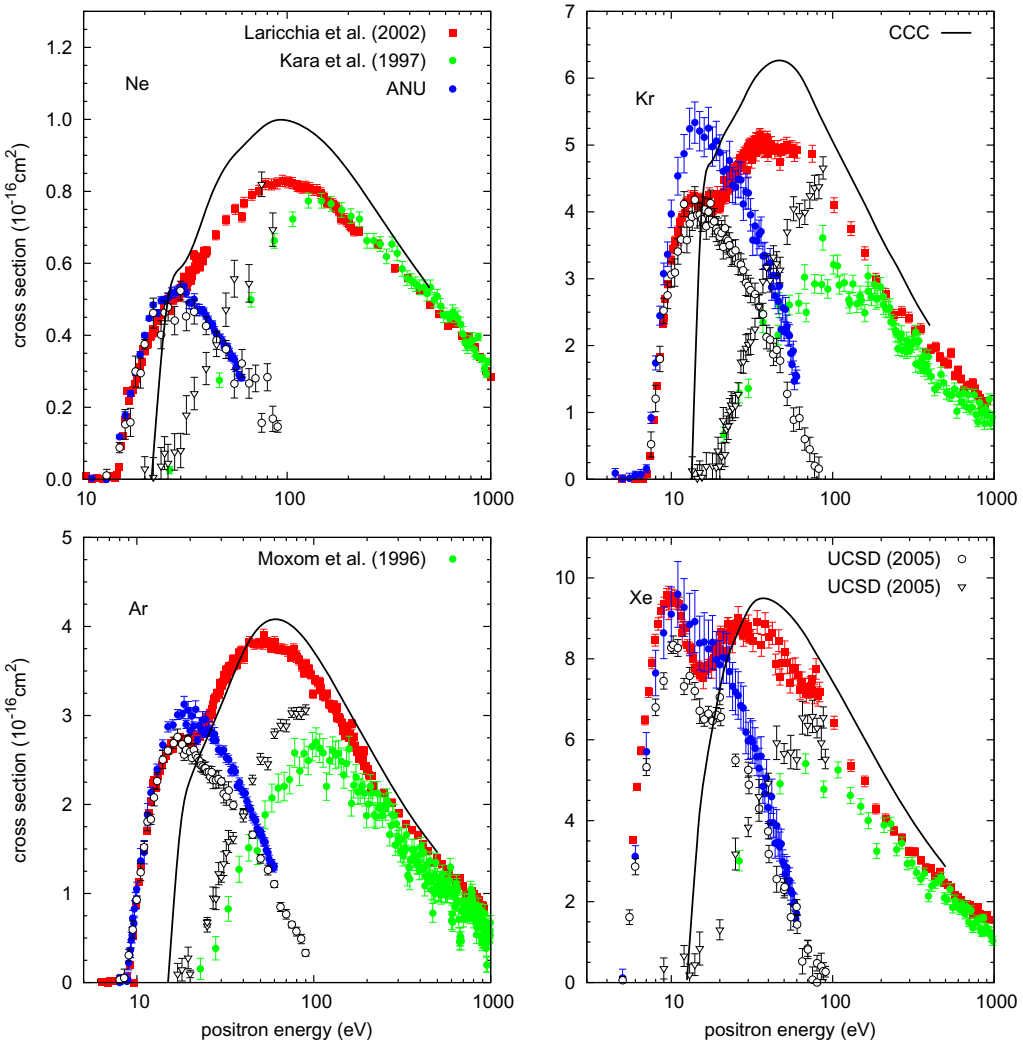

Figure 4. Total Ps-formation, direct ionization and ionization (sum of the other two) cross sections for positron scattering from Ne, Ar, Kr and Xe. The experimental data are from [12–18]. The present CCC calculations are described in the text.

the rapid rise is that just above the ionization threshold the calculated TICS is dominated by Ps formation, which is already very large. At energies below the ionization threshold, the experimental TICS values are the Ps-formation cross sections. There is slight variation between the several experimental data sets for the Ps-formation and direct ionization cross sections. Consequently, it is difficult to say if the systematic overestimation of the experiment by the CCC theory is a reflection of the structure approximations. We note that the calculated TICS include only single-electron ionization from the outer p-shell, while experimental results also include ionization from the inner orbitals. The small discrepancy may be related to the normalization of the data of [16] at large energies to the electron-impact ionization cross sections of [62]. Previous normalization to the measurements of [63] leads to higher experimental TICS values and better agreement with the CCC results.

Finally, we note that a comparison of figures 2 and 4 shows that the TICS are roughly a factor of two less than the corresponding TCS. For electron scattering there is at least an order of magnitude difference in the same (low to intermediate) energy region. This is of course due to the attractive nature of the positron–electron interaction. So while the term 'inert gas' is certainly appropriate for interactions with electrons, these targets are as reactive as any other for interactions with positrons.

4. Conclusions

We have developed a single-center CCC method for positron scattering from noble gases. The target structure is modeled as six p-electrons above an inert Hartree–Fock core. Only one-electron excitations from the outer p^6 shell are considered. The use of a Sturmian basis makes it possible to take into account ionization and Ps formation at energies above the ionization threshold. Virtual effects at energies below the Ps formation are also accurately treated, allowing for the estimation of the scattering lengths. The overall agreement with experiment is very encouraging.

Future development of the method will aim to take into account Ps-formation channels directly via a two-center CC expansion. Relativistic generalization of the method will also be considered, which should be advantageous in investigating the positron impact on the heavy noble gases (Xe, Rn). A more accurate structure model that relaxes the frozen-core approximation is also desirable and will be adopted in the near future.

Acknowledgments

We thank Nella Laricchia, James Sullivan and Luca Chiari for providing their data in electronic form. We acknowledge support from the Australian Research Council and the Australian National Computational Infrastructure Facility and its Western Australian node iVEC.

References

[1] Utamuratov R, Kadyrov A S, Fursa D V, Bray I and Stelbovics A T 2010 *J. Phys. B: At. Mol. Opt. Phys.* **43** 125203
[2] Murtagh D J, Cooke D A and Laricchia G 2009 *Phys. Rev. Lett.* **102** 133202
[3] Caradonna P, Sullivan J P, Jones A, Makochekanwa C, Slaughter D, Mueller D W and Buckman S J 2009 *Phys. Rev.* A **80** 060701
[4] Campbell C P, McAlinden M T, Kernoghan A A and Walters H R J 1998 *Nucl. Instrum. Methods* B **143** 41
[5] Igarashi A, Toshima N and Shirai T 1996 *Phys. Rev.* A **54** 5004
[6] Murtagh D J, Szluinska M, Moxom J, Reeth P V and Laricchia G 2005 *J. Phys. B: At. Mol. Opt. Phys.* **38** 3857
[7] Knudsen H, Brun-Nielsen L, Charlton M and Poulsen M R 1990 *J. Phys. B: At. Mol. Opt. Phys.* **23** 3955
[8] Fromme D, Kruse G, Raith W and Sinapius G 1986 *Phys. Rev. Lett.* **57** 3031
[9] Kauppila W E, Stein T S, Smart J H, Dababneh M S, Ho Y K, Downing J P and Pol V 1981 *Phys. Rev.* A **24** 725
[10] Zecca A, Chiari L, Trainotti E, Fursa D, Bray I and Brunger M 2011 *Eur. Phys. J.* D **64** 317
[11] Zecca A, Chiari L, Trainotti E, Fursa D, Bray I and Brunger M 2012 *J. Phys. B: At. Mol. Opt. Phys.* **45** 015203

[12] Jones A C L *et al* 2011 *Phys. Rev.* A **83** 032701
[13] Makochekanwa C *et al* 2011 *Phys. Rev.* A **83** 032721
[14] Machacek J R *et al* 2011 *New J. Phys.* **13** 125004
[15] Marler J P, Sullivan J P and Surko C M 2005 *Phys. Rev.* A **71** 022701
[16] Laricchia G, Reeth P V, Szluinska M and Moxom J 2002 *J. Phys. B: At. Mol. Opt. Phys.* **35** 2525
[17] Kara V, Paludan K, Moxom J, Ashley P and Laricchia G 1997 *J. Phys. B: At. Mol. Opt. Phys.* **30** 3933
[18] Moxom J, Ashley P and Laricchia G 1999 *Can. J. Phys.* **74** 367
[19] Marler J P, Surko C M, McEachran R P and Stauffer A D 2006 *Phys. Rev.* A **73** 064702
[20] McEachran R P, Ryman A G and Stauffer A D 1978 *J. Phys. B: At. Mol. Opt. Phys.* **11** 551
[21] Sin Fai Lam L T 1982 *J. Phys. B: At. Mol. Opt. Phys.* **15** 143
[22] Baluja K L and Jain A 1992 *Phys. Rev.* A **46** 1279
[23] Parcell L A, McEachran R P and Stauffer A D 2002 *Nucl. Instrum. Methods* B **192** 180
[24] Campeanu R, McEachran R and Stauffer A 1996 *Can. J. Phys.* **74** 544
[25] Gilmore S, Blackwood J E and Walters H R J 2004 *Nucl. Instrum. Methods* B **221** 129
[26] Dzuba V A, Flambaum V V, Gribakin G F and King W A 1996 *J. Phys. B: At. Mol. Opt. Phys.* **29** 3151
[27] Kernoghan A A, Robinson D J R, McAlinden M T and Walters H R J 1996 *J. Phys. B: At. Mol. Opt. Phys.* **29** 2089
[28] Kadyrov A S and Bray I 2002 *Phys. Rev.* A **66** 012710
[29] McAlinden M T and Walters H R J 1992 *Hyperfine Interact.* **73** 65
[30] Bartschat K, Hudson E T, Scott M P, Burke P G and Burke V M 1996 *J. Phys. B: At. Mol. Opt. Phys.* **29** 115
[31] Badnell N R 2008 *J. Phys. B: At. Mol. Opt. Phys.* **41** 175202
[32] Zatsarinny O and Bartschat K 2008 *Phys. Rev.* A **77** 062701
[33] Heller E J and Yamani H A 1974 *Phys. Rev.* A **9** 1201
[34] Yamani H A and Fishman L 1975 *J. Math. Phys.* **16** 410
[35] Konovalov D A and Bray I 2010 *Phys. Rev.* A **82** 022708
[36] Bray I and Stelbovics A T 1992 *Phys. Rev.* A **46** 6995
[37] Bray I and Fursa D V 1995 *J. Phys. B: At. Mol. Opt. Phys.* **28** L197
[38] Fursa D V and Bray I 2008 *Phys. Rev. Lett.* **100** 113201
[39] Fursa D V and Bray I 1997 *J. Phys. B: At. Mol. Opt. Phys.* **30** 757
[40] Bray I, Fursa D V, Kheifets A S and Stelbovics A T 2002 *J. Phys. B: At. Mol. Opt. Phys.* **35** R117
[41] Fursa D V and Bray I 1995 *Phys. Rev.* A **52** 1279
[42] Bray I 1994 *Phys. Rev.* A **49** 1066
[43] Norcross D W and Seaton M J 1976 *J. Phys. B: At. Mol. Opt. Phys.* **9** 2983
[44] Fursa D V and Bray I 1997 *J. Phys. B: At. Mol. Opt. Phys.* **30** 5895
[45] Caves T C and Dalgarno A 1972 *J. Quant. Spectrosc. Radiat. Transfer* **12** 1539
[46] Hafner P and Schwarz W H E 1978 *J. Phys. B: At. Mol. Opt. Phys.* **11** 2975
[47] Ralchenko Y, Kramida A E, Reader J and NIST ASD Team 2011 *NIST atomic spectra database (version 4.10)*
[48] Canter K F, Coleman P G, Griffith T C and Heyland G R 1973 *J. Phys. B: At. Mol. Opt. Phys.* **6** L201
[49] Stein T S, Kauppila W E, Pol V, Smart J H and Jesion G 1978 *Phys. Rev.* A **17** 1600
[50] Charlton M, Laricchia G, Griffith T C, Wright G L and Heyland G R 1984 *J. Phys. B: At. Mol. Opt. Phys.* **17** 4945
[51] Sinapius G, Raith W and Wilson W G 1980 *J. Phys. B: At. Mol. Opt. Phys.* **13** 4079
[52] Karwasz G P, Pliszka D and Brusa R S 2006 *Nucl. Instrum. Methods* B **68** 68
[53] Coleman P G, McNutt J D, Diana L M and Burciaga J R 1979 *Phys. Rev.* A **20** 145
[54] Jaduszliwer B and Paul D A L 1974 *Appl. Phys.* **3** 281
[55] Kauppila W E, Stein T S and Jesion G 1976 *Phys. Rev. Lett.* **36** 580
[56] Dababneh M S, Kauppila W E, Downing J P, Laperriere F, Pol V, Smart J H and Stein T S 1980 *Phys. Rev.* A **22** 1872

[57] Jay P M and Coleman P G 2010 *Phys. Rev.* A **82** 012701
[58] Mitroy J, Bromley M W J and Ryzhikh G G 2002 *J. Phys. B: At. Mol. Opt. Phys.* **35** R81
[59] Surko C M, Gribakin G F and Buckman S J 2005 *J. Phys. B: At. Mol. Opt. Phys.* **38** R57
[60] Gribakin G F and Ludlow J 2004 *Phys. Rev.* A **70** 032720
[61] McEachran R P, Stauffer A D and Campbell L E M 1980 *J. Phys. B: At. Mol. Opt. Phys.* **13** 1281
[62] Sorokin A A, Shmaenok L A, Bobashev S V, Möbus B, Richter M and Ulm G 2000 *Phys. Rev.* A **61** 022723
[63] Krishnakumar E and Srivastava S K 1988 *J. Phys. B: At. Mol. Opt. Phys.* **21** 1055